Open access • Proceedings Article • DOI:10.1190/1.1822322

Composite refraction-reflection stack sections: Tracing faults in the Atlantic coastal plain sediments — Source link

Cahit Çoruh, John K. Costain, Dale E. Stephenson

Institutions: Virginia Tech, Westinghouse Electric

Published on: 01 May 1993 - Seg Technical Program Expanded Abstracts (Society of Exploration Geophysicists)

Topics: Coastal plain

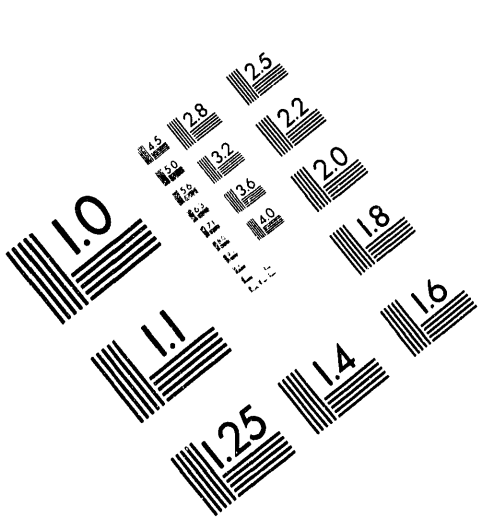

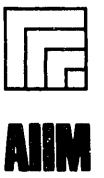

Association for Information and Image Management
1100 Wayne Avenue, Suite 1100
Silver Spring, Maryland 20910
301/587-8202

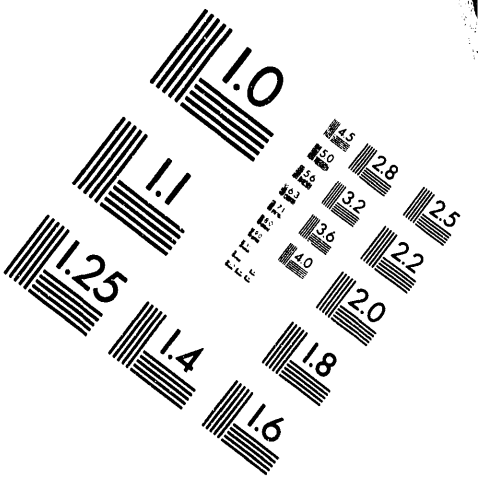

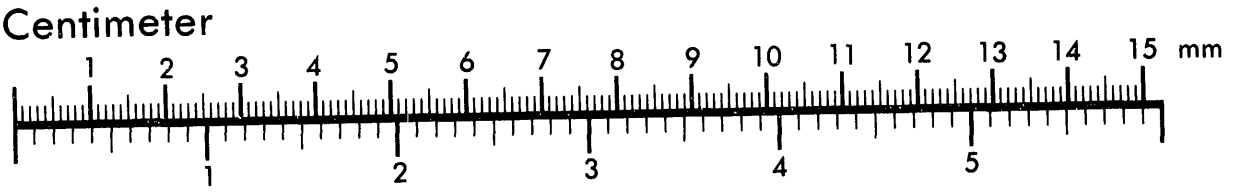

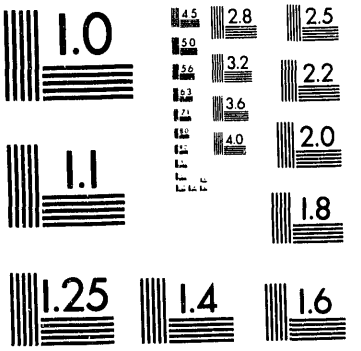

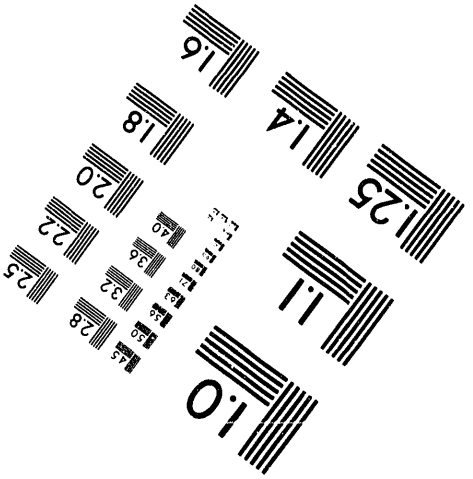

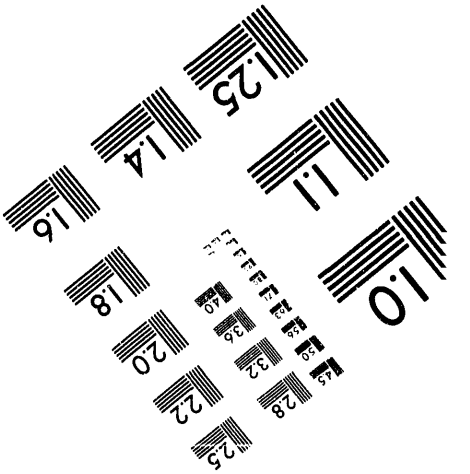

1 of 1

WSRC-MS-93-179

COMPOSITE REFRACTION-REFLECTION STACK SECTIONS: TRACING FAULTS IN THE ATLANTIC COASTAL PLAIN SEDIMENTS (U)

by D. E. Stephenson

Westinghouse Savannah River Company
Savannah River Site
Aiken, South Carolina 29808

Other Authors:

C. Caruh
Virginia Tech
Blacksburg, VA
J. K. Costain
(VT)

A paper proposed for Presentation
at/in the Society of Exploration Geophysicists Annual Meeting
Washington, DC
09/26-30/93

DISCLAIMER

Composite Refraction-Reflection Stack Sections: Tracing Faults in the Atlantic Coastal Plain Sediments

Cahit Çoruh and John K. Costain, Department of Geological Sciences, Virginia Tech, Blacksburg, Virginia 24061-0420
Dale E. Stephenson, Westinghouse Savannah River Company, Savannah River Technology Center, Aiken, South Carolina, 29808

SUMMARY

Seismic data from the Atlantic Coastal Plain are reprocessed and composite refraction-reflection stack sections produced to investigate basement faults that penetrate upward into Atlantic Coastal Plain sediments in South Carolina. Reprocessing recovered reflections from within the deep crust to the Moho as well as from within thin veneer (300 m) of the Atlantic Coastal Plain sediments. In addition to attempts to recover reflected arrivals from shallow depths, reprocessing was focused on shallow structures by recovering refracted head wave arrivals using refraction stack sections discussed in this paper. Portions of the seismic lines that cross interpreted faults are reprocessed with emphasis on the enhancement of shallow seismic events using a mute scheme that minimizes loss of data and yields composite refraction and reflection stack sections. The refraction stack sections are produced by stacking the split-spread data (sorted by the mid-point coordinates) and applying a linear-move-out correction that transforms the refraction arrival times into intercept (delay) times. Velocities necessary for the correction were obtained from constant-velocity test panels using the linear-move-out correction. The refraction stacks produced extremely good refracted signals representing horizons that are correlated with corresponding reflections and/or synthetic seismograms from well log data. The correlation formed the basis for constructing the composite refraction-reflection stack sections that are then used to determine the upward penetration of faults imaged in crystalline basement, the Dunbarton Triassic basin and the Cretaceous sediments of the Atlantic Coastal Plain. The faulting, in general, is not limited to the Triassic Dunbarton basin which is interpreted to be bounded by reverse (at the NW) faults. Other faults imaged in the sediments and extending upward from the basement are generally reverse faults. Deformation without faulting is imaged in Tertiary sediments and is associated with some of the deeper faults that penetrate the sediments. Displacement imaged along faults decreases rapidly upward from the basement. The composite refraction-reflection stack sections exhibit that the depth of upward penetration of the faults varies; most of them are associated with deformation at times as small as 50 ms two-way time (≃25 m), while one fault (the ATTA) penetrates to depths that include a shallow refracted horizon. Imbricated upper crustal structures, the buried Triassic Dunbarton basin, and reverse and normal faults suggest that the subsurface is overprinted by compression followed by extension and later by compression.

INTRODUCTION

One of the major objectives of this paper is to discuss the use of shallow refracted arrivals to construct a composite refraction-reflection stack that allows better imaging of the subsurface at shallow depths. Conventional processing of multifold reflection data generally requires that refracted wave arrivals be discarded by the application of a mute. Here, we encourage the use of refracted waves using a stacking process similar to the conventional stacking process of reflected waves (Yilmaz, 1987). Seismic data recorded for reflection arrivals also include refracted arrivals in which the reflected wavefronts are represented by hyperbolic time-delays (normal moveout) on traces with increasing offset, while the refracted waves are represented by linear time-delays. Because the correction for normal moveout causes non-linear stretching, the refracted waves and stretched parts of traces are normally included in the mute scheme. We suggest using a combination of linear and non-linear corrections to recover both type of arrivals. Our attempts have resulted in additional data and information that can be used as a part of the interpretation (Laughlin, 1988; Sen, 1991; Çoruh and others, 1992). Information gained from the refracted arrivals allows interpretations about shallower structures that can not be imaged by reflected arrivals only.

The conventional interpretation of refraction data uses a single-fold approach and either planar or irregular refraction interfaces (Barry, 1967; Palmer, 1986, Lankston, 1989). Most techniques used for interpreting refraction traveltime-distance curves are derived from the concept of delay time. The refraction stack discussed here is also designed to utilize the delay times.—These are combined using multifold data in which traces are recorded with different offsets similar to common-mid-point reflection ensembles.

The traveltime t_x for a critically refracted wave arriving at a source-receiver distance x (Figure 1) is

$$t_x = t_0 + \frac{x}{V_2} \tag{1}$$

where t_0 is the delay- or intercept-time and V_2 is velocity of the second layer. The delay-time is

$$t_0 = \frac{2h}{V_1}\cos i_c \tag{2}$$

where h and V_1 are thickness and velocity of the first layer, respectively; and

$$\cos i_c = \sqrt{1 - \left[\frac{V_1}{V_2}\right]^2} \tag{3}$$

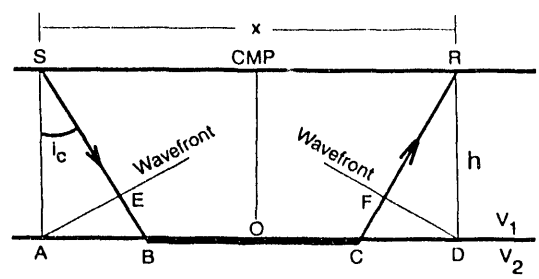

Figure 1. Critically refracted wave arrival: CMP is the mid-point between source and receiver. $t_{SF} = SE/V_1$ and $t_{FR} = FR/V_1$ are the source and receiver terms of the delay time, respectively.

Delay time t_0 consists of a source term ($t_{SF} = SE/V_1$) that is the time it takes the critically refracted wavefront to travel from the source point to the refractor with an angle of incidence i_c and a receiver term ($t_{FR} = FR/V_1$) that is the traveltime for the critically refracted wavefront to travel from the refractor to the receiver (Figure 1). The delay time, therefore, is the two-way traveltime for the critically refracted wavefront from source to refractor and then to a receiver. Since the delay time is obtained from Eq (1) by defining $x = 0$, Figure 2 is obtained by moving the critically refracted raypaths without modifying the critical angle of incidence i_c to simulate $x = 0$. In Figure 2 the source and receiver points are put together at the mid-point between the source and receiver locations in Figure 1. The linear time difference between the arrival time of refracted waves at an offset x and the delay time is called refraction moveout (RMO) at offset x, Figure 3. Application of the refraction moveout transforms the arrival time of the raypaths given in Figure 1 into the arrival time of the raypaths shown in Figure 2. Reduction of the arrival time of a critically

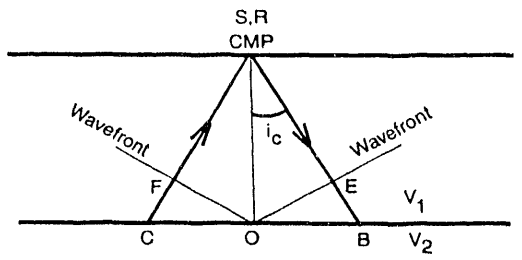

Figure 2. **Critically refracted wave arrival after refraction moveout correction:** The source and receiver points are moved to CMP point $t_{SF} = SE/V_1$ and $t_{FR} = FR/V_1$ are the source and receiver terms of the delay time, respectively. Figure represents the critically refracted planar wavefront to travel from CMP point to point O on the refractor and back to CMP point on the surface.

refracted wave at an offset is transformed into a delay time by subtracting the linear refraction moveout from the arrival time. From Figure 2, the relation between the refraction delay time and two-way zero-offset reflection time (T_0) shown in Figure 3 is

$$T_0 = \frac{t_0}{\cos i_c} \tag{4}$$

where $T_0 \geq t_0$. So, the refraction delay times can be converted into the reflection times by the cosine transformation. Now, let us look at multifold refracted wave arrivals in a common-mid-point ensemble.

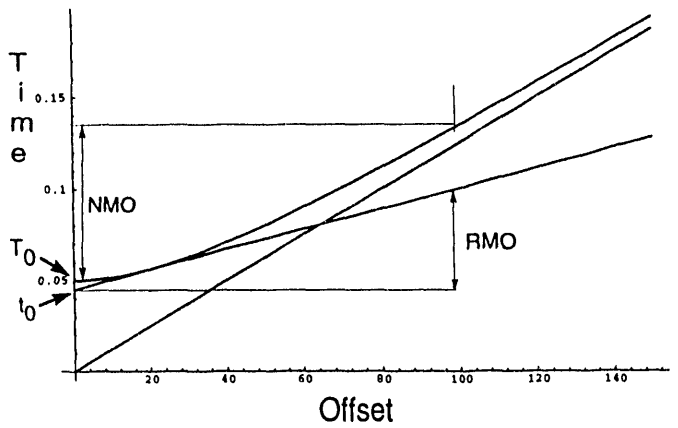

Figure 3. **Definition of linear refraction and hyperbolic reflection moveout:** RMO and NMO are the linear refraction and hyperbolic reflection moveouts at an offset x_5.

REFRACTION STACK

Multifold reflection data acquisition also results in multifold refracted wave raypath coverage because source and receiver pairs used are symmetric about a common-mid-point (CMP), as shown in Figure 4. This figure represents split-spread recorded traces sorted by the common-mid-point coordinates. Common-mid-point gathers used to prepare traces for stacking the reflected waves can be considered common refractor surface (CRS) ensembles for the refracted arrivals. CRS ensembles sorted by offset exhibit arrival times delayed by the linear refraction moveout. As shown in Figure 4 there are multi refracted raypaths covering the same surface. The delay times for these raypaths can be combined to represent the delay time for the common-mid-point (CMP). This geometry indicates that the delay time obtained by summing the delay times related to these raypaths results in a smoothing effect. The number of raypaths covering the same part of the refractor is a maximum at the center beneath the common-mid-point (CMP), and tapers out in both directions. It is obvious that a data set comprised of the combined delay times from an irregular refractor will be a function of the layer thickness beneath the common-mid-point. Removal of the refraction moveout would reduce all arrival times in a CRS ensemble to a common delay time, as shown in Figure 5. After the correction for refraction moveout, all the refracted wavelets will appear at the same time if the refractor is planar and velocities are constant. If the refractor is irregular, the refracted wavelets will appear around an average delay time. These observations form the basis for using the common refraction surface ensembles after correcting for the linear refraction moveout. These ensembles are the input used to form the refraction stacks which are then spliced with the reflection stacks.

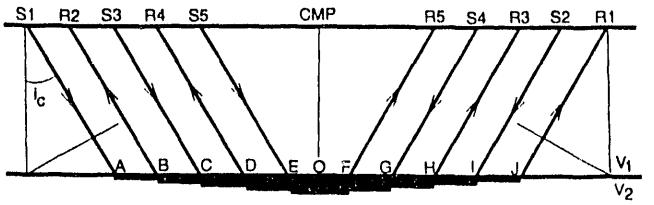

Figure 4. **Multifold critically refracted wave arrivals:** Multi-offset split-spread data sorted by the mid-point coordinates forms ensambles with the common-refraction-surface raypaths that show the maximum folding beneath the CMP point while the number of common-raypaths tapers out in both directions.

The refraction stack sections are constructed in the (x, t_0)-domain and are therefore suitable for direct interpretation. In contrast to the conventional use of refracted arrivals, the refraction stack utilizes first arrivals as well as later arrivals in data sets. The processing flow of a refraction stack is similar to a conventional processing flow for reflected arrivals. Refractor velocity information required to apply the refraction moveout correction can be obtained by velocity analysis schemes that use the linear moveouts. A general processing flow to produce a refraction stack from a multifold data set might include: refraction datum statics, amplitude balancing, sorting data sets into common-refraction-surface ensembles by mid-point coordinates, determination of refractor velocities, correcting the common-refraction-surface ensembles for the refraction linear moveout, stacking by summing the traces of the common-refraction-surface ensembles, amplitude balancing and filtering. This list might also include mute schemes if one would prefer to be selective.

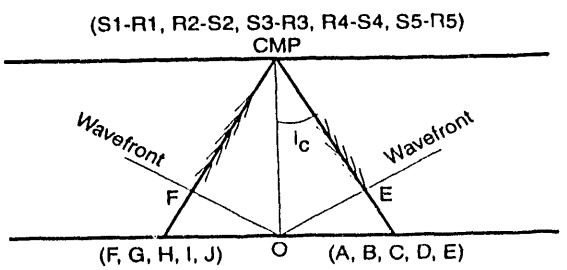

Figure 5. **Multifold critically refracted wave arrivals after RMO correction:** The raypaths in Figure 1 are moved to represent the critically refracted raypaths after refraction moveout correction. As 5-fold data, 5-pairs of source-receiver points are moved to point CMP, resulting in 5 down-going and 5 up-coming critically refracted wavefronts.

The multifold refraction data may be represented by

$$f_k(t) = r_k(t - RMO_k) + n_k(t) \quad (5)$$

where $r_k(t - RMO_k)$ is the refracted wave at an offset corresponding to trace counter k and $n_k(t)$ is noise. The trace, $g_N(t)$, obtained from N-fold refraction stack data can be represented by

$$g_N(t) = \sum_{k=1}^{N} f_k(t + RMO_k) \quad (6)$$

or

$$g_N(t) = \sum_{k=1}^{N} [r_k(t + RMO_k - RMO_k) + n_k(t + RMO_k)]$$

$$g_N(t) = \sum_{k=1}^{N} [r_k(t) + n_k(t + RMO_k)]$$

If the refracted wavelets representing different offsets are the same $r(t)$ for N-fold data, then the data that represent the refracted event at delay time t_r can be written as

$$g_N(t) \simeq Nr(t) + \sum_{k=1}^{N} n_k(t + RMO_k) \quad (8)$$

From this symbolic representation it is obvious that the refraction stack will enhance the refracted events while attenuating the noise. The stacking processes can also be used to scan for the velocity required for the refraction moveout correction. In the case of a planar sub-horizontal refractor, and independent of the recording style, the velocity will be the refractor velocity, which is

$$V_2 = \frac{V_1}{\sin i_c} \quad (9)$$

In the case of a dipping refractor and split-spread recording the velocity will be the average of the apparent velocities from down-dip and up-dip shooting that is

$$V_2 \simeq 0.5 \left[\frac{V_1}{\sin i_c - \alpha} + \frac{V_1}{\sin i_c + \alpha} \right] \quad (10)$$

In the case of dipping-refractor and one-sided recording the velocity will approximate either down-dip or up-dip apparent velocity, depending on the direction of the line and the recording style.

Although there is a strong smoothing effect because of refraction stacking, the portion of the refractor that contributes to the stack with the maximum number of wavelets is centered about the common-mid-point, and represents a relatively small area. The refraction stacked traces from the CRS ensembles represent two-way traveltimes (delay times) for critically refracted travel paths around the common-mid-point and therefore can reveal subsurface structures. For refraction stacking, the only velocity necessary is the refractor velocity, V_2. If the refraction delay times are to be converted into two-way reflection times, then, there is also the need for the velocity (V_1) of the first layer in order to define i_c. This conversion becomes more critical when the contrast between seismic velocities is larger.

Refraction-reflection stack sections are compared in Figure 6. The stack section on the left in Figure 6 was originally recorded and processed to interpret subsurface faults that penetrate upward from the upper crust into the overlying sediments of the Atlantic Coastal Plain in South Carolina. Interpretations resulting from this processing revealed subsurface faults that penetrate upward into the Coastal Plain sediments. Recognition of the deeper faults made it necessary to determine the upward penetration depth of the faults in order to determine the latest tectonic activity that produced displacement in the area. We carried out reprocessing that was targeted to recover shallower reflections than those in the seismic section on the left in Figure 6. It was possible to recover additional shallower reflections that helped to determine the upward penetration of the faults more accurately as shown on the right in Figure 6. Interpretation of the new results showed that the border fault between Triassic basin sediments and crystalline basement penetrated upward to as shallow a depth as the shallowest recovered reflection. It was necessary to trace this fault and others to shallower depths to determine fault offset. Examination of the data sets acquired for reflected arrivals showed that there were also sufficient refracted arrivals in the data suitable for refraction stacking. Velocity analysis carried out using constant velocity panels verified that there were recoverable arrivals. The refraction stacks obtained enabled us to image shallower structures than those recovered in the reflection stack sections. The composite refraction and reflection stack section shown on the right in Figure 6 has the same input data originally used to produce the section on the left in the same Figure. Similar results from other data sets will be discussed at the meeting. The refraction stacks produced extremely good refracted signals (Figure 6), and originate from horizons that correlate with corresponding reflections and/or synthetic seismograms from well log data. The correlations form the basis for constructing the composite refraction-reflection stack sections that are used to determine the upward penetration of faults imaged in crystalline basement, the Dunbarton Triassic basin and the Cretaceous Atlantic Coastal Plain sediments in South Carolina. In general, the faulting in the area is not limited to the Triassic Dunbarton basin, which is interpreted to be bounded by reverse (at the NW) and normal (at the SE) faults. There are other reverse faults imaged in the sediments that extend from the basement upward into the sediments. Deformation without faulting imaged in Tertiary sediments is associated with some of the deeper faults that penetrate the sediments. Displacement imaged along faults decreases rapidly upward from the basement. The composite refraction-reflection stack sections indicate that the depth of upward penetration of the faults varies; most of the faults are associated with deformation at times as small as 50 ms two-way time (≃25 m). One fault (the ATTA) penetrates to shallower depths that include the refracted horizon. Imbricated upper crustal structures, the buried Triassic Dunbarton basin and reverse and normal faults suggest that the subsurface structures have experienced compression followed by extension and later by compression again.

Different schemes might be used to produce composite refraction-reflection stack sections. We suggest three methods to combine refracted and reflection stack data:

- Refraction and reflection stack data sets can be generated by utilizing linear refraction and hyperbolic reflection moveout corrections separately. The two data sets with equivalent arrival times can then be combined together to produce the composite stack data.
- The linear refraction moveout and hyperbolic reflection moveout can be utilized in the same algorithm to produce the composite stack data. A reference two-way zero-offset time can control the type of moveout correction and different mute schemes if necessary.
- A τ-p domain processing can be used to separate the refracted and reflected arrivals before linear and hyperbolic moveout corrections are made.

CONCLUSION

Data sets acquired for reflected arrivals also include refracted arrivals. In contrast to the conventional approach, we discard parts of data sets as little as possible. The resulting stack sections show that attempting to retain as much recorded data as possible can make a difference in the recovered

reflections. In addition to keeping reflected arrivals we suggest that refracted arrivals should be included in the final stack sections. The refracted events recovered in the composite refraction-reflection stack sections can help to image and interpret shallower structure for different purposes. The example shown in this paper is used to trace the upward penetration depth of the faults that extend upward into the Atlantic Coastal Plain sediments from deeper upper crustal structures. Shallow structures imaged by the refracted waves can also be used to minimize the effect of long wavelength statics on the reflected arrivals.

ACKNOWLEDGMENTS

The feasibility of refraction stacks on different data sets has been tested at Virginia Tech since 1985. We thank Kenneth Laughlin, Ashok K. Sen, and William J. Domoracki for their contributions in testing the approach on different data sets.

REFERENCES

Barry, K.M., 1967, Delay time and its application to refraction profile interpretation, in Seismic Refraction Prospecting: ed., Musgrave, A.W., Tulsa, Soc. Explor. Geophys., pp. 348-361.

Coruh, C., Sen, A.K., Domoracki, W.J., Costain, J.K., Stephenson, D.E., and Stieve, A.L., 1992, Faulting in the Coastal Plain sediments: Seismic images from composite reflection and refraction stack sections, Geological Society of America Abstracts With Programs, v. 24, p. 9-10.

Lankston, R. W., 1989, The seismic refraction method: A viable tool for mapping shallow targets into the 1990s: Geophysics, 54, 1535-1542.

Laughlin, K. J., 1988, Interpretation of refraction and reflection stack data over the Brevard Fault Zone in South Carolina: M.S. Thesis in Geophysics, Virginia Tech, 42 pp.

Palmer, D., 1986, Refraction Seismics the lateral resolution of structure and seismic velocity: eds., Helbig, K. and Treitel, S., London, Geophysical Press, 269 p.

Sen, A.K., 1991, Removing near-surface effects in seismic data: Application for determination of faults in the Coastal Plain sediments: M.S. Thesis in Geophysics, Virginia Tech, 98 pp.

Yilmaz, O., 1987, Seismic Data Processing: Investigations in Geophysics Series Volume 2, ed., S. M. Doherty, Tulsa, OK, Society of Exploration Geophysicists, 526 pp.

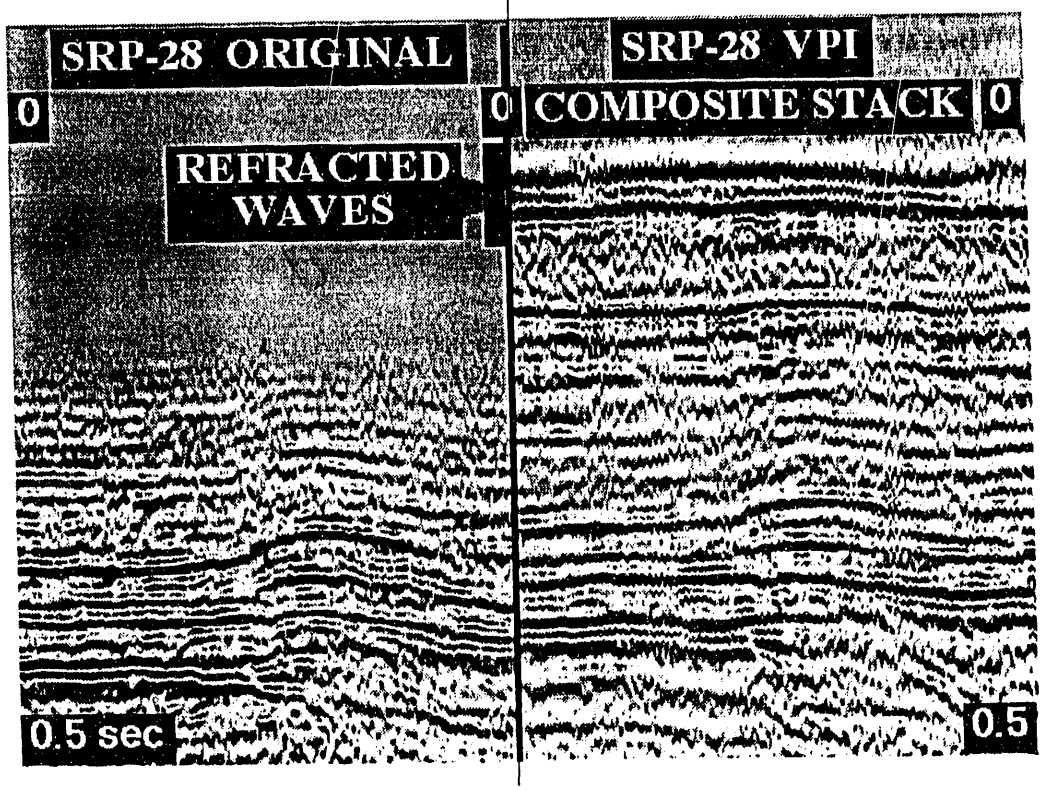

Figure 6. Comparison of reflected and composite refracted-reflected stack data: Left: Reflection stack obtained by conventional processing to trace the upward extent of faults penetration from the upper crust into the Atlantic Coastal Plain sediments. Right: Composite refraction-reflection stack obtained by special processing to recover shallower reflections and refractions. The difference between the right and left speaks for itself.

DATE
FILMED
8/16/93
END